Short- and long-latency components of the eCAP reveal different refractory properties

Dong, Y.; Briaire, J.J.; Stronks, H.C.; Frijns, J.H.M.

Hearing Research 420 (2022) 108522

Contents lists available at ScienceDirect

Hearing Research

journal homepage: www.elsevier.com/locate/heares

Short- and long-latency components of the eCAP reveal different refractory properties

Yu Dong[a,b], Jeroen J. Briaire[a], H. Christiaan Stronks[a], Johan H.M. Frijns[a,c,*]

[a] ENT-Department, Leiden University Medical Centre, PO Box 9600, 2300, RC Leiden, the Netherlands
[b] Department of Psychology, Beijing Forestry University, Beijing, China
[c] Leiden Institute for Brain and Cognition, PO Box 9600, 2300, RC Leiden, the Netherlands

ARTICLE INFO

Article history:
Received 6 October 2021
Revised 4 May 2022
Accepted 14 May 2022
Available online 16 May 2022

Keywords:
Cochlear implants
Auditory nerve
Sensorineural hearing loss
Refractory recovery
Electrically evoked action potential
Speech perception

ABSTRACT

Background: The refractory recovery function (RRF) measures the electrically evoked compound action potential (eCAP) in response to a second pulse (probe) after masking by a first pulse (masker). This RRF is usually used to assess the refractory properties of the electrically stimulated auditory nerve (AN) by recording the eCAP amplitude as a function of the masker probe interval. Instead of assessing eCAP amplitudes only, recorded waveforms can also be described as a combination of a short-latency component (S-eCAP) and a long-latency component (L-eCAP). It has been suggested that these two components originate from two different AN fiber populations with differing refractory properties. The main objective of this study was to explore whether the refractory characteristics revealed by S-eCAP, L-eCAP, and the raw eCAP (R-eCAP) differ from each other. For clinical relevance, we compared these refractory properties between children and adults and examined whether they are related to cochlear implant (CI) outcomes.
Design: In this retrospective study, the raw RRF (R-RRF) was obtained from 121 Hi-Focus Mid-Scala or 1 J cochlear implant (Advanced Bionics, Valencia, CA) recipients. Each R-eCAP of the R-RRF was split into an S-eCAP and an L-eCAP using deconvolution to produce two new RRFs: S-RRF and L-RRF. The refractory properties were characterized by fitting an exponential decay function with three parameters: the absolute refractory period (T); the saturation level (A); and the speed of recovery from nerve refractoriness (τ), i.e., a measure of the relative refractory period. We compared the parameters of the R-RRF (R_T, R_A, $R\tau$) with those obtained from the S-RRF (S_T, S_A, $S\tau$) and L-RRF (L_T, L_A, $L\tau$) and investigated whether these parameters differed between children and adults. In addition, we examined the associations between these parameters and speech perception in adults with CI. Linear mixed modeling was used for the analyses.
Results: We found that T_R was significantly longer than S_T and L_T, and S_T was significantly longer than L_T. R_A was significantly larger than S_A and L_A, and S_A was significantly larger than L_A. Also, $S\tau$ was significantly longer in comparison to $R\tau$ and $L\tau$, but no significant difference was found between $R\tau$ and $L\tau$. Children presented a significantly larger S_A and L_A and a shorter R_T in comparison to adults. Shorter $S\tau$ was significantly associated with better speech perception in adult CI recipients, but other parameters were not.
Conclusion: We demonstrated that the two components of the eCAP have different refractory properties and that these also differ from those of the R-eCAP. In comparison with the R-eCAP, the refractory properties derived from the S-eCAP and L-eCAP can reveal additional clinical implications in terms of the refractory difference between children and adults as well as speech performance after implantation. Thus, it is worthwhile considering the two components of the eCAP in the future when assessing the clinical value of the auditory refractory properties.

1. Introduction

Cochlear implantation is currently the standard of care for the auditory rehabilitation of patients with severe to profound sensorineural hearing loss. A cochlear implant (CI) transforms a

* Corresponding author at: ENT Department, Leiden University Medical center, P.O. Box 9600, 2300 RC Leiden, The Netherlands.
E-mail address: J.H.M.Frijns@lumc.nl (J.H.M. Frijns).

https://doi.org/10.1016/j.heares.2022.108522

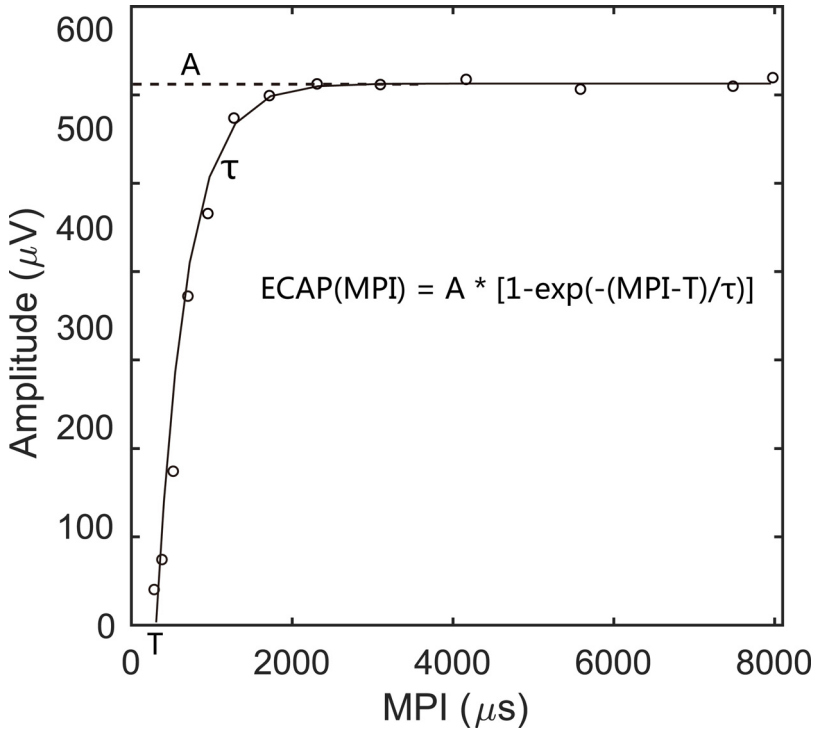

Fig. 1. The eCAP refractory recovery function (RRF) as fitted using an exponential model with three parameters (i.e., T, A, and τ). The eCAP is in response to a second stimulus pulse (the probe), following a first pulse (the masker), separated by a given MPI. eCAP: electrically evoked compound action potential. MPI: masker probe interval. T is the absolute refractory period (in μs); A is the maximum eCAP amplitude at the maximum saturation level (in μV), and τ is the recovery time constant during the relative refractory period (in μs). MPI: masker probe interval.

sound signal into electrical stimuli that directly activate the auditory nerve (AN) inside the cochlea (Hughes, 2012). Previous studies reported that the neural refractoriness of the AN can affect its capability of accurately encoding temporal information (e.g., Gray, 1967; Wilson et al., 1994; Brown et al., 1990; Boulet et al., 2016; He et al., 2017) and is relevant to the functionality of the AN as well as speech perception (e.g., Stypulkowski and van den Honert, 1984; Wilson et al., 1994; He et al., 2017).

A common approach to exploring the refractory characteristics of the AN is to measure the refractory recovery function (RRF) of the electrically evoked compound action potential (eCAP) using a masker-probe artifact cancelation paradigm. In this paradigm, two pulses are applied, and the eCAP in response to the second pulse (the probe) is measured as a function of the masker probe interval (MPI). The RRF can be obtained by plotting the eCAP amplitudes as a function of MPI (Miller et al., 2000; Morsnowski et al., 2006; Hey et al., 2017). Refractoriness arising from the first pulse (the masker) results in a masking of the eCAP triggered by the probe. In this paradigm, the eCAP is characterized by the amplitude of the main peaks, namely the difference between the first negative peak (N1) and the first positive peak (P1). As shown in Fig. 1, the refractory properties of the AN can be obtained by fitting the RRF with an exponential function using three parameters: (1) the absolute refractory period (T), indicating the time during which a neural spike cannot be produced regardless of the magnitude of the stimulus; (2) the eCAP amplitude at the maximum saturation level (A), representing the maximum eCAP amplitude evoked by the probe after a sufficiently long MPI; and (3) the relative refractory period (τ), during which time the auditory nerve fiber can be activated, but only by relatively high stimulus levels (e.g., Morsnowski et al., 2006; Botros and Psarros, 2010; He et al., 2017).

However, the method used in previous studies to assess the AN refractoriness is controversial (e.g., Miller et al., 2000, 2001; Morsnowski et al., 2006), because in this paradigm, the eCAP is characterized only by the amplitude of the main peaks. In considering the morphology of eCAPs, previous studies have observed two different types of eCAP waveforms (e.g., Van den Honert and Stypulkowski, 1984; Lai and Diller, 2000; Ramekers et al., 2015; van de Heyning et al., 2016; Dong et al., 2020). These waveforms can consist of either one negative and one positive peak or of two positive peaks that are similar in shape but differ in latencies (P1 and P2) (e.g., Lai and Dillier, 2000; He et al., 2017). The raw eCAP waveform (R-eCAP) can be described as a combination of a short-latency component (S-eCAP) and a long-latency component (L-eCAP). They may be attributed to a separate neural response of part of the AN fiber (ANF) population (Ramekers et al., 2015; Strahl et al., 2016; Konerding et al., 2020; Dong et al., 2020). This two-component concept was also supported by a single-fiber recording study in cats (Van den Honert and Stypulkowski, 1984). More importantly, the two groups of neural responses can be related to the survival and functional conditions of the AN. For instance, Strahl et al. (2016) found that the ratio between S-eCAP and L-eCAP increased with the neural degeneration of the AN in the guinea pig. Based on results recorded in cats, Stypulkowski and van den Honert (1984) reported that L-eCAP represents propagated neural responses initiated on the dendritic processes of the AN fibers and the characteristic non-monotonicity of the RRF curve of the L-eCAP may be indicative diagnostically for the degeneration of the peripheral processes of the AN fibers. However, previous studies have not investigated whether the S-eCAP and L-eCAP reveal different auditory refractory properties. We assumed that these two components arise from two different populations of ANFs, and therefore they may exhibit different refractory characteristics. Thus, in this study, we investigated the auditory refractory properties of the AN underlying the S-eCAP and L-eCAP.

Variation in terms of refractory characteristics of the AN between individuals and between different etiologies of deafness has been previously reported (e.g., Gantz et al., 1994; Fulmer et al.,

2011; Van Eijl et al., 2017; He et al., 2017). Due to factors such as the duration of deafness and the maturation of the AN, differences in auditory refractory characteristics may be expected between young and adult CI users. For instance, in an animal study, the absolute refractory period of individual rat auditory neurons increased with the duration of deafness (Shepherd et al., 2001, 2004). Thus, a shorter absolute refractory period in children was anticipated, as children may presumably experience a shorter duration of deafness before being implanted than the average adult implant recipient (Gordon et al., 2002). To our knowledge, this has only been investigated by Carvalho et al. (2015), who reported no difference in refractory characteristics between children and adults except for the maximum saturation level. More importantly, earlier studies have not explored whether the auditory refractory characteristics underlying S-eCAP and L-eCAP in adults differ from or are the same as those in children.

Previous studies have attempted to explore whether the AN's speed of recovery from refractoriness is associated with the speech outcomes of adult CI recipients. These studies have not reported the effects of the absolute refractory period and saturation level on speech recognition, and results on the speed of recovery have been inconsistent. Some studies have reported that faster recovery from refractoriness derived from R-eCAP associates with better speech performance scores (Brown et al., 1990; Kiefer et al., 2001; Battmer et al., 2005; Fulmer et al., 2011), while other studies did not find such a relation (Abbas and Brown, 1991; Turner et al., 2002; Batter et al., 2005; Lee et al., 2012). One likely reason behind the incongruity is that previous studies only focused on the R-eCAP without considering the S-eCAP and L-eCAP separately.

Based on the above considerations, the first goal of the present study was to explore whether different refractory properties could be identified for the two components of the R-eCAP waveforms. To this end, the eCAP waveforms of the raw RRFs (R-RRFs) in a large group of CI patients were split into an S-eCAP and L-eCAP using iterative deconvolution (Dong et al., 2021). Using this method, two derived RRFs (S-RRF and L-RRF) were obtained from the R-RRFs, and the T, A, and τ parameters of the R-RRF, S-RRF and L-RRF were compared. Then, we investigated the potential clinical relevance of these refractory parameters, including (1) whether the parameters of the S-RRF, L-RRF, and R-RRF in children differed from those obtained from adult CI recipients and (2) whether these parameters can be indicative of speech outcomes in adult CI recipients.

2. Materials and methods

2.1. Patients

This was a retrospective study based on RRFs obtained from 121 bilaterally deaf patients with little residual hearing (implantation criteria in the Netherlands are relatively stringent). The RRFs were recorded as part of the clinical routine during cochlear implantation surgery at the Leiden University Medical center (Leiden, the Netherlands) between January 2010 and December 2015, but were not always available because of time constraints in the operating theater. All the included patients received a HiRes90K device (Advanced Bionics, Valencia, CA), either with a Mid-Scala or a 1 J electrode array. Sixteen patients were excluded during data processing, because of poor signal quality of eCAPs and failure of RRF fitting (see Data Recordings and Analysis). The remaining 105 patients were included for further analyses (Table 1).

Table 1
Patient demographics.

Number of Patients	105
Cochlear implant type (n)	
HiRes90K 1 J	14
HiRes90K Mid-Scala	91
Age (years)	
Children (<16 years)	42
Mean age ± SD (years)	5.2 ± 3.6
Adults (> = 16 years)	63
Mean age ± SD (years)	61.8 ± 15.9
Etiology (n)	
Medication	1
Meningitis	7
Otosclerosis	2
Congenital/Hereditary	35
Other/Unknown	60

SD represents standard deviation.

2.2. Data recordings

The RRF recordings were conducted using a masker-probe artifact cancelation paradigm (Miller et al., 2000), which was provided by the Research Studies Platform Objective Measures software (RSPOM, Advanced Bionics, Valencia, CA). A schematic of the paradigm is shown in Fig. 2. In this method, the masker-probe interval (MPI) systematically varies from 300 to 8000 μs. The evoked eCAP response to the partially masked probe (trace A) is recorded by a contact that is two electrodes apical to the stimulus. As the MPI increases, the AN gradually recovers from the refractory status induced by the masker, which leads to larger eCAPs at longer MPIs in trace A. The neural response and artifact evoked by the masker are measured (trace B). The artifact and the eCAP evoked by the probe pulse are derived by subtracting trace B from trace A (i.e., A-B). The reference MPI is set to minimize the neural response evoked by the probe pulse (trace C) (Morsnowski et al., 2006). Subtracting trace D from trace C (i.e., C-D) yields the artifact induced by the probe. The difference between the two derived traces (i.e., (A-B)-(C-D)) is the eCAP evoked by the first probe. The RRF was obtained by plotting the eCAP amplitudes as a function of MPIs. In the present study, the RRF recording was obtained using 13 MPIs (300, 398, 538, 721, 969, 1293, 1734, 2327, 3114, 4181, 5603, 7500, 7995 μs).

The electrode arrays used in this study consisted of 16 contacts that were numbered from 1 to 16 in apical-to-basal order. RRF measurements were obtained at an apical electrode (E3), a middle position (E8), and a basal position (E14). Due to time constraints in the operating theater, not all contacts could be recorded in all patients. Three stimulation electrode sites were recorded for 64 patients, two stimulation electrode sites (E3, E8) were recorded for 29 patients, and one stimulation site (E3) was recorded for 28 patients. The eCAPs were evoked using monopolar, charge-balanced, cathodic-first biphasic pulses (32 μs/phase) with a constant probe level of 500 clinical units (CUs). The probe level was measured in CUs, where CU equals pulse duration (μs) · amplitude (μA)/78.7. The number 78.7 is a unitless correction factor defined by the CI manufacturer (e.g., De Jong et al. 2020). The eCAPs were recorded with a sampling rate of 56 kHz and a gain of 300. Raw eCAP recordings were low-pass filtered with a cutoff frequency of 8 kHz. N1 was defined as the minimum within the period from 180 to 490 μs, and P1 was the maximum from 470 to 980 μs after the end of stimulation. The eCAP amplitude was defined as the voltage difference between P1 and N1. The noise level was set to the average of the tail section of the recorded eCAP, i.e., the last 30 samples of the response. The signal-to-noise ratio was defined as the eCAP amplitude divided by the noise (Biesheuvel et al., 2018). eCAPs were in-or excluded using an automatic method programmed using MATLAB (Mathworks 2019a, Natick, MA, USA), including two criteria: (1) the eCAP amplitude had to be larger than 30 μV and (2) the SNR had to exceed +15 dB. If the eCAPs did not meet both of these criteria, they were excluded. After the automated analysis, the identified N1 and P1 peaks were visually inspected. To ensure

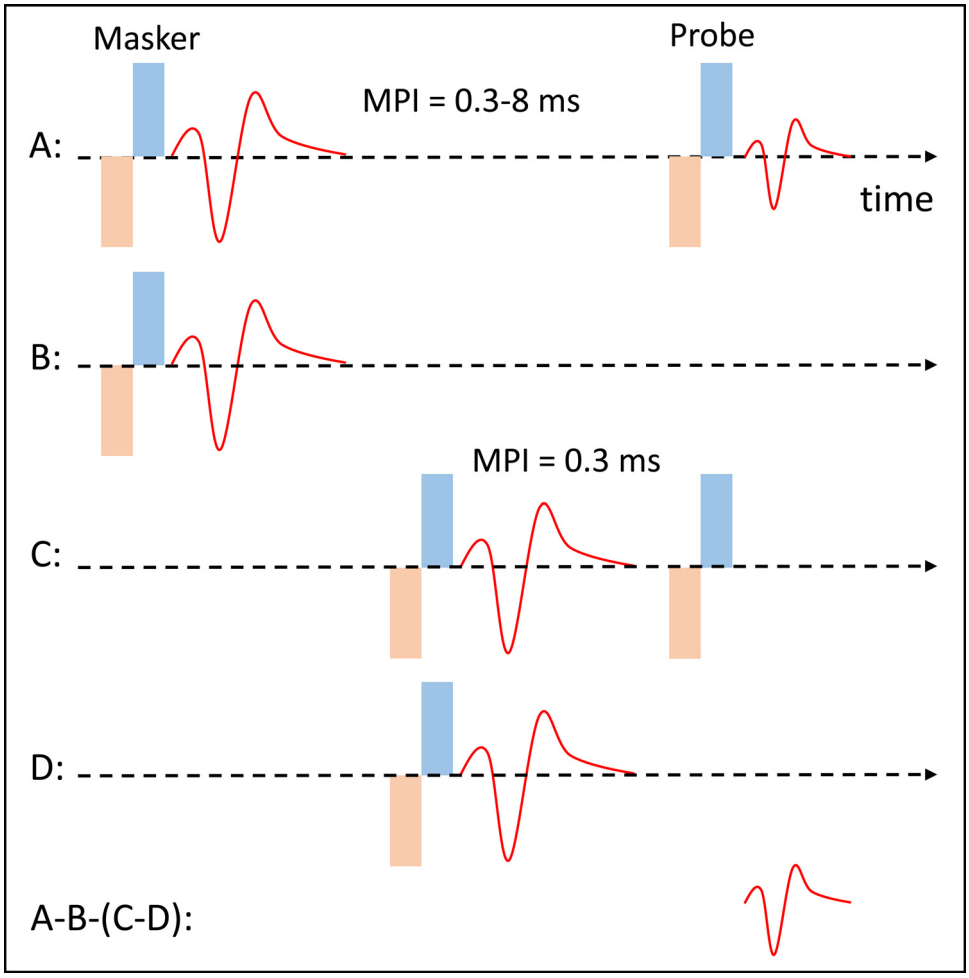

Fig. 2. A schematic illustration of the masker-probe artifact cancelation paradigm for measuring the eCAP refractory recovery function. Red solid lines indicate eCAP response. Colored rectangles indicate biphasic current pulses. Adapted from Miller et al. (2000). eCAPs: electrically evoked compound action potentials. MPI: masker probe interval.

reliability, a stimulation site was excluded if more than 3 out of 13 eCAP waveforms of each R-RRF sequence did not meet these two criteria. As a result, 35 stimulation sites (including 11 sites at E3, 10 sites at E8, and 14 sites at E14) were excluded and the remaining 243 R-RRFs were used for extracting the S-RRF and L-RRF.

2.3. Analysis

2.3.1. Extracting the s-eCAP and l-eCAP from the recorded eCAP

Under the assumption that each ANF generates the same unitary response, the R-eCAP can be described as a convolution of the unitary response with a compound discharge latency distribution consisting of two Gaussian components (for details, see Dong et al., 2021). The two Gaussian components represent the discharge latency distribution of the S-eCAP and the L-eCAP, respectively. To extract the S-eCAP and L-eCAP from the R-eCAP, two steps were performed. First, combined with a human unitary response, the compound discharge latency distribution was derived from the R-eCAP using an iterative deconvolution model (Dong et al., 2020, 2021). Second, the S-eCAP and L-eCAP were simulated by convolving the first and second components of the compound discharge latency distribution with the human unitary response, respectively. The summation between the S-eCAP and L-eCAP mathematically equals the R-eCAP. We examined if this summation can accurately simulate the R-eCAP waveform by calculating the normalized root mean square error using MATLAB (Mathworks 2019a, Natick, MA, USA). Then, we determined the amplitudes of the S-eCAP and L-eCAP in the same manner as the R-eCAP amplitude. The S-RRF and L-RRF were obtained by plotting the amplitudes of S-eCAP and L-eCAP as a function of MPIs.

2.3.2. Deriving the refractory properties from R-RRF, S-RRF, and L-RRF

An exponential decay function was used to characterize the R-RRF, S-RRF, and L-RRF (e.g., Matsuoka et al., 2001; Morsnowski et al., 2006; Fulmer et al., 2011; Boulet et al., 2016).

$$ECAP\ (MPI) = A * \left(1 - e^{\left(-\frac{(MPI-T)}{\tau}\right)}\right) \quad (1)$$

T is the absolute refractory period (in μs), i.e., the minimum MPI for which an eCAP can be triggered by the probe. The amplitude recovers to the saturation level A (in μV) with a speed-of-recovery time constant τ (in μs). That is, τ represents the relative refractory period, reflecting the speed of recovery from relative refractoriness. R_T, R_A, and $R\tau$ denote the parameters of R-RRF; S_T, S_A and $S\tau$ are those of S-RRF; and L_T, L_A and $L\tau$ are those of L-RRF. These parameters were calculated by fitting the R-RRF, S-RRF, and L-RRF using a least-squares curve fit with the Levenberg-Marquart algorithm using MATLAB (Mathworks 2019a, Natick, MA, USA). As the absolute refractory period cannot be shorter than 0 µs, a stimulation site was excluded if any one of the parameters (R_T, S_T, or L_T) was smaller than 0 μs, indicating a fitting error. As a result, 28 stimulation sites (including 9 sites at E3, 7 sites at E8, and 12 sites at E14) were excluded, and the remaining 215 sites originating from 105 patients were included for further statistical analyses.

2.4. Speech perception

Refractory properties were correlated to speech recognition performance 1 year after implantation defined as the word and phoneme correct rate. This performance measure was routinely evaluated for the adult CI recipients. From 17 patients the speech recognition scores were unavailable and they had to be excluded from analysis, including 7 prelingually deaf patients, 2 reimplanted patients, and 8 patients for whom speech test scores were unavailable for unknown reasons. Among them, 4 were preemptively implanted without extensive pre-operative screening, because of meningitis. The remaining 46 patients (41 with a Mid-Scala and 5 with a 1 J electrode array) were used in further analysis. The HiRes processing strategy from Advanced Bionics was applied to all patients. The speech material was presented at 65 dB SPL in the free field in a quiet listening environment. In the rare cases where the residual hearing in the unaided contralateral ear could contribute to speech recognition, the contralateral ear was plugged. All speech testing was conducted in a soundproof room, using a calibrated sound speaker in a frontal position at a meter distance. The standard Dutch speech test of the Dutch Society of Audiology, consisting of phonetically balanced monosyllabic (CVC) word lists, was applied (Bosman and Smoorenburg, 1995). To enhance test reliability, four lists of 11 CVC words were administered. The number of words and phonemes that were correct was determined.

2.5. Statistics

In the present study, we used linear mixed modeling (LMM) for statistical analyses, because (1) LMMs have the advantage that they can account for random effects (i.e., variability within and between patients (Gałecki and Burzykowski, 2013)), (2) LMMs can account for missing data that do not have to be random (Molenberghs et al., 1997; Fitzmaurice et al., 2004) and, importantly, (3) it allowed us to enter all the RRF data across electrodes into one model, substantially increasing statistical power. We first tested whether the short and long-latency components of the eCAP revealed different refractory characteristics and whether they differed from those revealed by the raw eCAP waveform. To this end, three LMMs were constructed with each of the refractory parameters (i.e., T, A, and τ) as the dependent variable. To test whether the parameters derived from S-RRF and L-RRF differed from each other and from the ones obtained from R-RRF, a categorical fixed factor was introduced that reflected whether T, A, and τ were obtained from R-RRF, S-RRF, or L-RRF. An example model for parameter A is given as follows:

$$A = RSL + contact + 1\,subject\,ID \quad (2)$$

where A is the dependent variable; RSL is the categorical variable with three levels (R, S, and L) corresponding to R-RRF, S-RRF, and R-RRF; the contact with the levels (E3, E8, and E14) is entered as a fixed-effect variable; and subject ID is entered as a random categorical variable, including a random intercept (Brauer and Curtin, 2018). The significance level of each comparison was adjusted to 0. 017 using post hoc Bonferroni-corrected multiple comparisons t-testing (0.05 divided by 3 comparisons).

Then, we evaluated the clinical relevance of the refractory parameters derived from R-RRF, S-RRF, and L-RRF. To compare the refractory characteristics between children and adults, nine LMMs were constructed that incorporated the following dependent variables: R_T, R_A, $R\tau$, S_T, S_A $S\tau$, L_T, L_A, and $L\tau$. In these analyses, the 105 patients were classified into a child group ($<=$ 16 years, n = 42) and an adult group (>16 years, n = 63) by age (see Table 1). This categorical variable was entered as a fixed effect factor with two levels (i.e., pediatric and adult). The electrode contact number and subject ID were entered in the same way as Eq. (2). In these analyses, both the pre- and postlingually deaf patients were included, because a previous study showed that there is no significant difference in the refractory properties between the two groups (Carvalho et al., 2020).

In addition, we investigated whether the refractory parameters obtained from R-RRF, S-RRF, and L-RRF are related to the speech perception of adult CI recipients. Again, nine individual LMMs were constructed in which the adults' speech performance dependency on the refractory parameters R_T, S_T, L_T, R_A, S_A, L_A, $R\tau$, $S\tau$, and $L\tau$ were tested, respectively. Normally, the outcome measure (speech recognition) would be entered as the dependent. However, multiple measures for the refractory metrics were available, because three electrode contacts were recorded, but only a single speech score was present. To allow the use of all the available data per refractory parameter and hence increase statistical power, we used a reverse approach where R_T, S_T, L_T, R_A, S_A, L_A, $R\tau$, $S\tau$, and $L\tau$ were entered as the dependent variable, and the monosyllabic word score as a fixed covariate in each LMM. The electrode contact and subject ID were included as a fixed-effect variable and a random variable, respectively (see Eq. (2)). Additionally, the relationship between phoneme score and the refractory parameters was evaluated in the same way.

The normality of the residuals assumption of each individual LMM in this study was tested with the qqnorm (residuals(A)) using R (e.g., Crawley, 2012; Harrison et al., 2018; Schielzeth et al., 2020) and no violation of this assumption was observed. LMM analyses were carried out using the lme4 package in R (version 3.6.1, The R Foundation for Statistical Computing, 2020).

3. Results

3.1. Extraction of S-eCAP and L-eCAP from R-eCAP

Each of the 2188 R-eCAP waveforms from 215 R-RRFs was split into an S-eCAP and an L-eCAP using iterative deconvolution. To test the validity of the deconvolution routine, the R-eCAPs were reconstructed from the S-eCAP and the L-eCAP by summation. The sum of the S- and L-eCAPs accurately reconstructed the R-eCAP, with median goodness of fit (i.e., the normalized root-mean-square error) of 91.7% (95% confidence interval: 89.5%–95.7%). A typical example of the extraction of the S-eCAP and L-eCAP is shown in Fig. 3. In this example, the summation of the S-eCAP and the L-eCAP matched the R-eCAP with a goodness of fit of 92.4%. One can directly see from this example that the latencies from the S-eCAP and L-eCAP are different, but also that the amplitude is far from that of the R-eCAP waveform. This illustrates that part of the response is canceled out of the summation of the responses due to the latency differences.

3.2. The refractory parameters derived from the R-RRF, S-RRF, and L-RRF

Table 2 shows a descriptive analysis of the refractory parameters extracted from the R-RRF, S-RRF, and L-RRF, including measurements of central tendency (mean and median), and dispersion (median deviation). An example of the exponential fitting of the R-RRF, S-RRF, and L-RRF is shown in Fig. 4.

To test whether the refractory parameters derived from R-RRF, S-RRF, and L-RRF differed from each other, three LMMs were constructed for which T, A, and τ were entered as the dependent variable, respectively. In addition, a fixed variable was included that indicated whether R-RRF, S-RRF, or L-RFF was tested. All three LMMs showed a significant main effect of this fixed, categorical variable (T: $F(2, 547) = 81.2$, $p<0.0001$; A: $F(2, 536) = 299$,

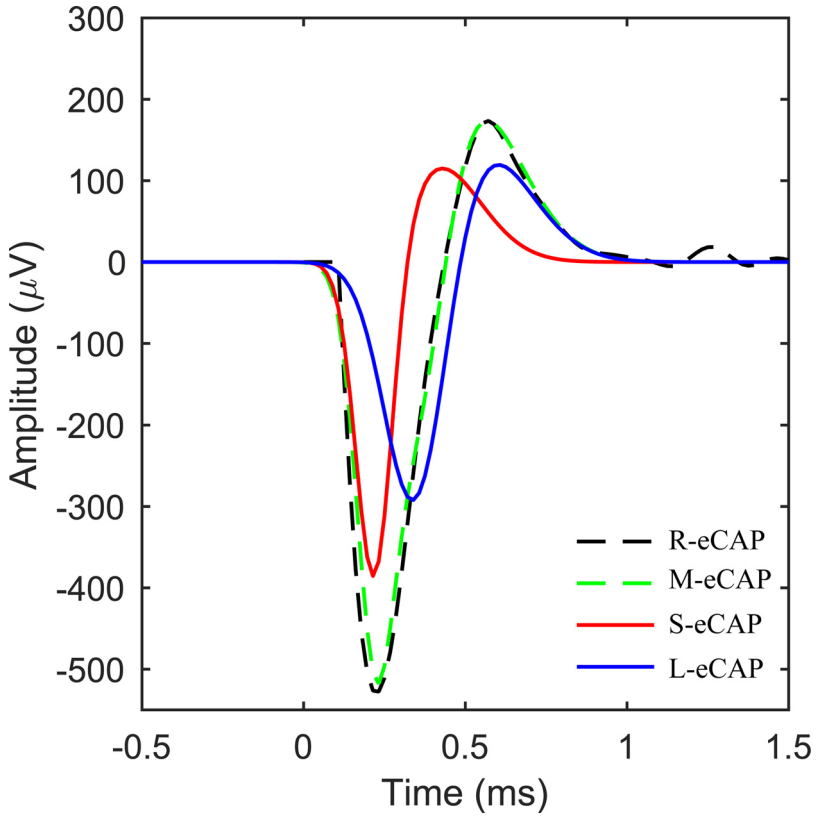

Fig. 3. A typical example of extracting the short-latency component (S-eCAP, the red solid line) and long-latency component (L-eCAP, the blue solid line) from the raw eCAP (R-eCAP, the black dashed line) of the raw eCAP refractory recovery function (R-RRF). The modeled eCAP (M-eCAP, the green dashed line) indicates the summation of the S-eCAP and the L-eCAP. eCAP: electrically evoked compound action potential.

Table 2
Descriptive results of the refractory parameters of the full sample, children, and adults. R-RRF, S-RRF, and L-RRF are the same as for Fig. 3. R_T, R_A, and $R\tau$ are for the R-RRF; S_T, S_A, and $S\tau$ are for the S-RRF; L_T, L_A, and $L\tau$ are for the L-RRF. MD represents the median absolute deviation.

Refractory Variables	Full -sample			Children			Adults		
	Median	Mean	MD	Median	Mean	MD	Median	Mean	MD
R_T (μs)	368	366	85	349	334	101	392	392	92.5
S_T (μs)	306	300	29	352	353	93.3	397	401	70.5
L_T (μs)	285	229	38	370	360	110	405	428	85.8
R_A (μV)	432	390	159	446	470	67	353	393	178
S_A (μV)	426	385	164	438	452	118	339	375	181
L_A (μV)	220	184	105	224	218	71.9	157	181	63.7
$R\tau$ (μs)	427	272	85	286	438	210	294	350	199
$S\tau$ (μs)	529	338	211	208	347	273	237	229	182
$L\tau$ (μs)	430	274	251	209	389	245	276	332	224

$p<0.0001$; and τ: $F(2537) = 4.1$, $p = 0.004$, respectively). The contact number showed a significant effect on parameter T ($p = 0.04$), A ($p<0.0001$) and τ ($p = 0.02$).

To compare how the refractory parameters T, A, and τ differed between the R-RRF, S-RRF, and L-RRF (see Eq. (2)), we used a post hoc *t*-test where the significance level was Bonferroni corrected to 0.017 (0.05 divided by 3 comparisons). For the absolute refractory period, R_T was significantly longer than S_T ($p<0.001$) and L_T ($p<0.001$), and S_T was significantly longer than L_T ($p<0.001$). Regarding saturation level, R_A was significantly larger than S_A ($p = 0.011$) and L_A ($p<0.0001$), and S_A was significantly larger than L_A ($p<0.0001$). For the speed of recovery, we found that $S\tau$ was significantly longer than $R\tau$ ($p<0.01$) and $L\tau$ ($p<0.01$), and no significant difference was observed between $R\tau$ and $L\tau$ ($p = 0.87$).

3.3. Comparisons of refractory parameters between children and adults

Table 2 shows the results of the descriptive analyses of the refractory parameters between children and adults, including central tendency (mean and median), and dispersion (median deviation). We tested whether children and adults had different refractory characteristics by constructing nine LMMs with R_T, R_A, $R\tau$, S_T, S_A, $S\tau$, L_T, L_A, and $L\tau$ entered as a dependent variable. For the absolute refractory period, only R_T in children was significantly shorter than those in adults ($F(1, 92.3) = 10.4$, $p = 0.002$). S_T ($F(1, 94.7) = 0.0003$, $p = 0.98$) and L_T ($F(1, 95) = 0.19$, $p = 0.66$) did not differ significantly between the two groups. Also, the saturation levels in children were significantly larger than those of adults

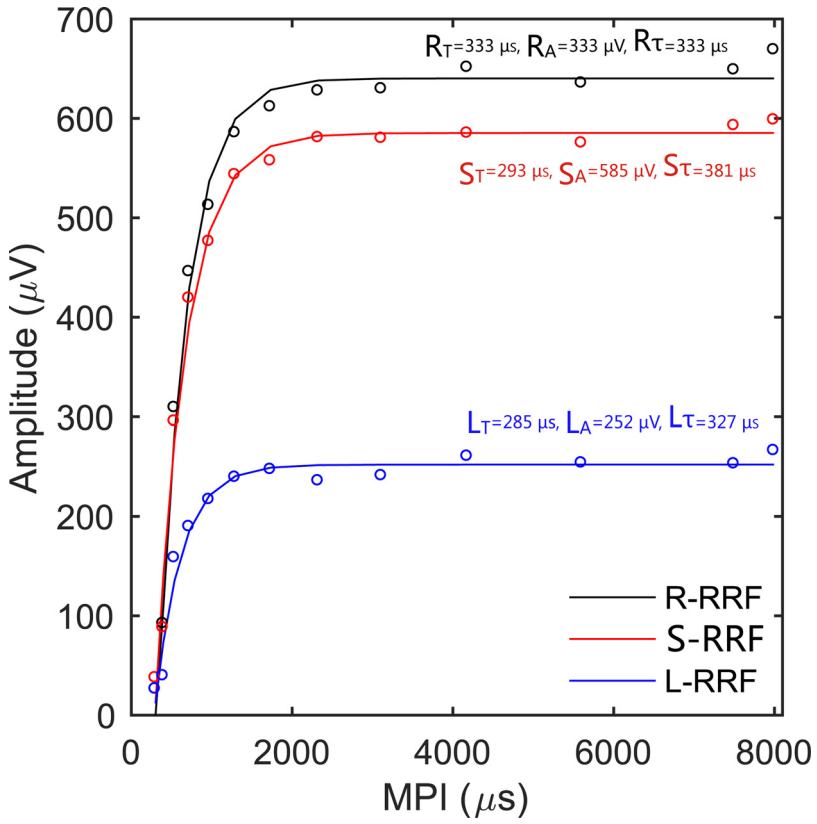

Fig. 4. Fitting the exponential model to the R-RRF, S-RRF, and L-RRF. R-RRF represents the recorded eCAP refractory recovery function; S-RRF and L-RRF represent the refractory recovery function of the short-latency and long-latency components in eCAPs. T is the absolute refractory period (in μs); A is the maximum eCAP amplitude at the maximum saturation level (in μV), and τ is the recovery time constant during the relative refractory period (in μs). R_T, R_A, and $R\tau$ are for the R-RRF; S_T, S_A, and $S\tau$ are for the S-RRF; L_T, L_A, and $L\tau$ are for the L-RRF. MPI: the masker-probe interval. R-eCAP, S-eCAP, and L-eCAP are the same as for Fig. 3.

R_A: $F(1, 96.5) = 5.0$, $p = 0.03$; S_A: $F(1, 97.8) = 4.4$, $p = 0.04$) except for L_A ($F(1, 102) = 4.1$, $p = 0.05$). Regarding the relative refractory period, no significant difference was observed between the two groups ($R\tau$: $F(1, 102.8) = 3.9$, $p = 0.05$; $S\tau$: $F(1, 101) = 0.8$, $p = 0.38$; and $L\tau$: $F(1, 105) = 0.9$, $p = 0.35$). The contact number showed a significant effect on parameters R_A, S_A, L_A and $R\tau$. Specifically, the R_A, S_A, and L_A became significantly smaller along the electrode contact in an apical to basal order (R_A: $F(2, 119.1) = 34.9$, $p<0.0001$; S_A: $F(2, 123.3) = 32.1$, $p<0.0001$; L_A: $F(2, 139.2) = 27.1$, $p<0.0001$, respectively). The $R\tau$ significantly increased along the electrode contact from the apex to the base ($F(2, 129.4) = 4.1$, $p = 0.02$). No significant effect of contact number on parameters R_T, S_T, L_T, $S\tau$, and $L\tau$ was found (all $p>0.05$).

We also investigated the correlation between the 9 refractory parameters and age both in the child group and adult group using the Spearman correlation coefficient. The significance level of each comparison was corrected to 0.0027 using Bonferroni correction (0.05 divided by 18 comparisons). No significant correlation was observed (all $p>0.0074$).

3.4. Relations between refractory parameters and speech perception

Nine LMMs were respectively constructed to evaluate the association between speech perception and the refractory parameters (R_T, S_T, L_T, R_A, S_A, L_A, $R\tau$, $S\tau$, and $L\tau$) in adult CI recipients by entering them as the dependent variable and the speech score as a fixed covariate in each model, respectively. The average word recognition score at the one-year follow-up in the 40 adult patients with CI was 58% words correct (range from 17% to 92%) and 72% phonemes correct (range from 46% to 98%). We found that only $S\tau$ was significantly and negatively associated with word recognition score ($F(1, 53.2) = 6.5$, $p = 0.017$) and phoneme score ($F(1, 51.2) = 3.1$, $p = 0.04$), taking contact location along the electrode array into consideration (Fig. 5). That is, patients with a higher speed of recovery of the S-eCAP tend to have better speech perception. However, regarding the remaining parameters, no significant associations were observed (all $p>0.2$). In these LMMs, the contact number showed that R_A, S_A, and L_A were significantly larger at the apical contact than at the middle or basal contact of the cochlea (R_A: $F(2, 62.9) = 22.6$, $p<0.001$; S_A: $F(2, 67.4) = 17.2$, $p<0.001$; L_A: $F(2, 69.1) = 29.8$, $p<0.001$, respectively). The contact number did not show a significant effect on the other parameters (all $p>0.1$).

4. Discussion

Earlier studies suggested that human eCAPs include a short-latency component and a long-latency component, which are thought to arise from two different populations of ANFs. In the present study, we corroborated these findings by demonstrating the presence of two separate components in the human eCAP that have refractory characteristics that differ significantly from each other and from the raw eCAP. The refractory properties derived from S-RRF and L-RRF turned out to be of clinical relevance, because they differed significantly between children and adults and were significantly correlated with speech perception after cochlear implantation.

4.1. The refractory properties derived from the R-RRF, S-RRF, and l-RRF

We observed that the mean value of R_T was 368 μs and the mean value of $R\tau$ was 427 μs (Table 2). Previous studies reported

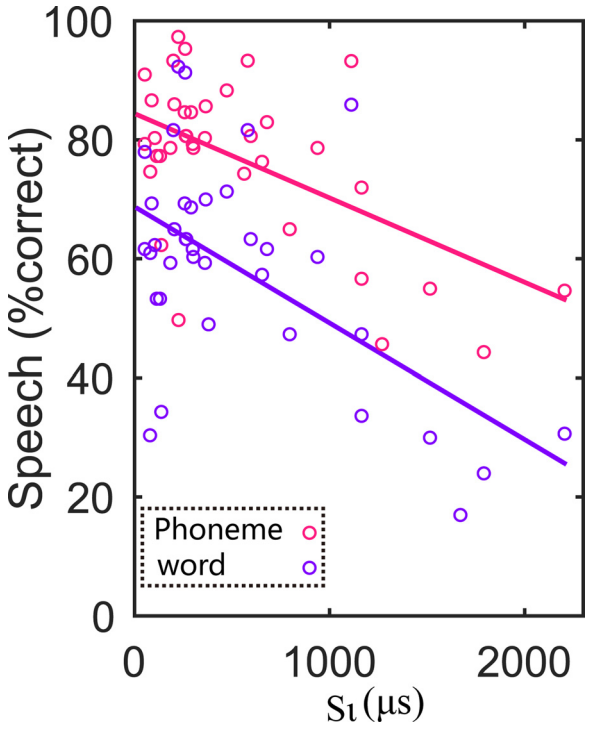

Fig. 5. Correlation between speech performance and the speed of recovery, Sτ. The scatterplot of recovery time constant (x-axis) plotted against the speech performance (y-axis).

mean or median values of R_T and Rτ ranging from 276 to 650 μs and from 410 to 1480 μs, respectively (Dynes, 1996; Bruce et al., 1999; Boulet et al., 2016; Viemes et al., 2016; Carvalho et al., 2020); thus, we conclude that our results fall within the ranges reported in the existing literature. The refractory parameters of the R-eCAP, S-eCAP, and L-eCAP all differed significantly from each other, with the sole exception being Rτ that did not significantly differ from Lτ. These findings support the notion that the short-latency and long-latency components of the eCAP can be attributed to two different populations of ANFs with different refractory characteristics. According to the above, compared with S-eCAP and L-eCAP, the use of the directly measured R-eCAP is not likely to give a meaningful representation of the refractory properties of the AN which may obscure potential clinical implications.

4.2. Refractory characteristics of the An in children and adults

The current study demonstrated a significantly shorter R_T and a significantly larger R_A in children than in adults, but there were no differences in Rτ between these groups. Our results were partially comparable with Carvalho et al. (2015), who found a significantly larger R_A in children than in adults. They did not find significant differences in R_T and Rτ between the two groups. Our results demonstrated that R-eCAP contains two different components with different refractory characteristics, and using S-eCAP and L-eCAP can lead to more accurate estimates of the refractory parameters. Thus, we further compared the refractory properties derived from the S-eCAP and L-eCAP between children and adults. Specifically, we only observed significant differences between the two groups for the S-RRF; namely, S_A was significantly larger in children. No significant differences between the two groups were observed for other parameters (S_T, L_T, L_A, Sτ, and Lτ). The result for S_A in our study was in line with the findings by Dong et al. (2020), who reported that a larger short-latency component of the compound discharge latency distribution, which is highly correlated to the eCAP amplitude, was observed in children. Gordon et al. (2002) also found higher eCAP amplitudes, i.e., 'A' values, in children compared with post-lingual adults. A possible explanation for the difference is that children have a larger number of healthy ANFs involved in S-eCAP than adults.

Age can reasonably be expected to correlate positively with the duration of hearing loss (e.g., Xi et al., 2004). Hence, adults can be expected to have more extended AN degeneration and a slower speed of recovery. We explored the relationship between age at implantation and the 9 refractory parameters, however, we did not find any significant correlations within the children or adult group. Our findings corroborate those of Lee et al. (2012), who report no significant differences in recovery time constants of the eCAP between the younger group and the elderly group. The results in the present study thus indirectly suggest that the duration of deafness appears to have little influence on the refractory properties. Earlies studies have, however, reported the duration of deafness to be an important factor affecting the refractory properties of the AN. Shepherd et al. (2004) found that the absolute refractory period of individual rat auditory neurons increased with the duration of deafness. Xi et al. (2004) reported that subjects with a short duration of deafness have faster recovery time constants than patients with a short duration of deafness.

Apart from the indirect correlation between duration of deafness and age, the lack of correlation between age and recovery characteristics in our study may have resulted from other factors as well, such as differences in the maturation state of the AN. Specifically, electrical stimulation with a cochlear implant in children affects the maturation of the AN (e.g., Xu et al., 1997) and hence can have affected recovery characteristics in this group depending on the time of implantation. Botros and Psarros (2010) proposed that a larger neural ANF population, rather than a longer duration of deafness, results in slower recovery and greater temporal responsiveness. Unfortunately, in the present study, the duration of deafness had too much missing data to correlate it with age or with therefractory properties of the AN. Taken together, there is still no agreement on whether the refractoriness differs between children and adults. To further address this issue, the state of maturation and degeneration of the ANF need to be taken into account in future studies, as well as the duration of deafness.

In the present study, we used $< = 16$ and >16 as an arbitrary criterion to divide the population into children and adults, respectively. To validate this criterion, the same analyses were performed by varying the criterion from 12 to 18 years in steps of 1 year, and no substantial differences in the main outcomes were identified. However, it should be pointed out that the duration of deafness does not necessarily correlate with age, especially for post-lingually deaf patients. For instance, the elder CI-recipients likely experienced a relatively short duration of deafness.

4.3. Effects of auditory refractory properties on speech perception

In the present study, we observed that the Rτ did not show a significant relationship with speech perception. Previous literature reports equivocal results in terms of the importance of Rτ for speech recognition outcomes with a CI (e.g., He et al., 2017). We argue that the derived measures of the speed of recovery, S-RRF and L-RRF, are better estimates than the R-RRF measures, as we found a significant association between Sτ and speech perception. One possible explanation was that two components in the eCAP originated from different populations of ANFs in terms of the degenerative state, maturation, and refractory characteristics. For instance, the S-eCAP may arise from a healthier group of fibers and the L-eCAP from a more degenerated group, representing different surviving and functional statuses (e.g., Ramekers et al., 2015; Konerding et al., 2020). Therefore, the two populations of ANFs can

affect speech perception differently, namely, the speed of recovery derived from the S-eCAP contributes significantly more to speech performance than that from L-eCAP. Importantly, the speed of recovery obtained by the conventional R-RRF using the raw eCAP amplitude does not predict performance, while considering the S- and L-eCAP separately proved to yield a more useful indicator for the CI outcomes. Furthermore, the results that the T and A parameters of R-RRF, S-RRF, and L-RRF did not correlate to speech perception suggested that they appear to be less essential factors for speech performance than $S\tau$. Therefore, we advise the use of the derived S-RRF and L-RRF components instead of R-RRF in future clinical practice to predict speech performance after implantation. However, various other (demographic) factors are involved in CI outcome, including, but not limited to, the degenerative state of the auditory nerve, maturation, preoperative performance, and duration of deafness (e.g., Shepherd and Hardie, 2001; Holden et al., 2013; Zhao et al., 2020).

4.4. Study limitations

A limitation of this study is that realistic refractory parameters of 29 RRFs (13.9%) could not be derived due to fitting errors. Morsnowski et al. (2006) also reported that 9 of 71 (12%) stimulation sites resulted in fitting errors. We believe that the possible reasons behind the failure may be the recording technique, as parameter estimates are likely to be sensitive to the number of data points; the MPI axis values; and the ANF density (Shepherd et al., 2004; Cohen, 2009; Boulet et al., 2016; He et al., 2017). The stability and validity of the exponential decay fitting of RRF (Eq. (1)) are sensitive to the number of data points and the MPI axis values, especially within the relative refractory period. For instance, when eCAPs cannot be detected due to background noise in the recording, the missing data likely result in a parameter discrepancy. It is possible that future studies, especially with additional MPIs within the relative refractory period, may refine the present estimates of the refractory characteristics of the whole nerve. In addition, uncertainty remains regarding the origins of the S-eCAP and L-eCAP (e.g., Strahl et al., 2016; Dong et al., 2020) and the physiological mechanism of the different refractory properties underlying the S-eCAP and L-eCAP. To further understand these issues, future studies with electrophysiological measures of the AN are warranted.

Another limitation of this study was the lacking data on the duration of deafness in the adults, and especially the children. This confounder may have affected the degenerative state of the AN and hence its refractory characteristics. We indirectly addressed this question by performing correlational analyses between refractory parameters and age, but further studies are needed to investigate this more conclusively. In terms of the predictive value of refractory characteristics of the AN on CI outcome, there were additional potential confounding factors including, but not limited to preoperative speech recognition, age, cognitive abilities, duration of deafness, number of active electrodes and speech coding strategy (e.g., Blamey et al., 1996; Holden et al., 2013; Zhao et al., 2020). It was outside the scope of this research to investigate these confounders comprehensively, because of the potential risk of underpowering the analyses or overfitting the data, given the limited number of available patients. To conclusively investigate the added value of the refractory properties of the auditory nerve, further studies will be required in the future.

5. Conclusions

In the current study, we demonstrated that the short-latency and long-latency components of the eCAP have different auditory refractory properties. The refractory properties of the two eCAP components differed between children and adults. Importantly, the speed of recovery, as obtained by the classical RRF method using the raw eCAP, did not predict speech performance. However, evaluating the two components of the eCAP separately proved to be indicative of speech performance after implantation. The collective results suggest that consideration should be given to the two components of the eCAP separately when the AN refractory characteristics are evaluated for clinical purposes.

CRediT authorship contribution statement

Yu Dong: Conceptualization, Methodology, Software, Formal analysis, Writing – original draft. **Jeroen J. Briaire:** Conceptualization, Methodology, Writing – review & editing, Supervision. **H. Christiaan Stronks:** Methodology, Writing – review & editing, Supervision. **Johan H.M. Frijns:** Writing – review & editing, Supervision.

Acknowledgments

The PhD study of the first author of the present study is financially supported by the China Scholarship Council. There are no conflicts of interest, financial or otherwise.

References

Abbas, P.J., Brown, C.J., 1991. Electrically evoked auditory brainstem response: refractory properties and strength-duration functions. Hear. Res. 51 (1), 139–147. doi:10.1016/0378-5955(91)90012-X.

Battmer, R.D., Lai, W.K., Dillier, N., Pesch, J., Killian, M.J., Lenarz, T., 2005. Correlation of NRT recovery function parameters and speech perception results for different stimulation rates. In: Abstracts of the Fourth International Symposium and Workshops on Objective Measures in Cochlear Implants, p. 21.

Biesheuvel, J.D., Briaire, J.J., Frijns, J.H., 2018. The precision of eCAP thresholds derived from amplitude growth functions. Ear. Hear. 39 (4), 701–711. doi:10.1097/AUD.0000000000000527.

Blamey, P., Arndt, P., Bergeron, F., Bredberg, G., Brimacombe, J., Facer, G., Larky, J., Lindström, B., Nedzelski, J., Peterson, A., Shipp, D., Staller, S., Whitford, L., 1996. Factors affecting auditory performance of postlinguistically deaf adults using cochlear implants. Audiol. Neurotol. 1 (5), 293–306. doi:10.1159/000259212.

Bosman, A.J., Smoorenburg, G.F., 1995. Intelligibility of Dutch CVC syllables and sentences for listeners with normal hearing and with three types of hearing impairment. Audiology 34 (5), 260–284. doi:10.3109/00206099509071918.

Botros, A., Psarros, C., 2010. Neural Response Telemetry Reconsidered: II. The Influence of Neural Population on the ECAP Recovery Function and Refractoriness. Ear & Hearing 31 (3), 380–391. doi:10.1097/AUD.0b013e3181cb41aa.

Boulet, J., White, M., Bruce, I.C., 2016. Temporal Considerations for Stimulating Spiral Ganglion Neurons with Cochlear Implants. JARO - J. Assoc. Res. Otolaryngol. 17 (1), 1–17. doi:10.1007/s10162-015-0545-5.

Brauer, M., Curtin, J.J., 2018. Linear mixed-effects models and the analysis of non-independent data: a unified framework to analyze categorical and continuous independent variables that vary within-subjects and/or within-items. Psychol. Methods 23, 389–411.

Brown, C.J., Abbas, P.J., Gantz, B., 1990. Electrically evoked whole-nerve action potentials: data from human cochlear implant users. J. Acoust. Soc. Am. 88 (3), 1385–1391. doi:10.1121/1.399716.

Bruce, I.C., Irlicht, L.S., White, M.W., O'Leary, S.J., Dynes, S., Javel, E., Clark, G.M., 1999. A stochastic model of the electrically stimulated AN: pulse-train response. IEEE Trans. Biomed. Eng. 46 (6), 630–637.

Carvalho, B., Hamerschmidt, R., Wiemes, G., 2015. Intraoperative neural response telemetry and neural recovery function: a comparative study between adults and children. Int. Arch. Otorhinolaryngol. 19, 10–15.

Carvalho, B., Wiemes, G.R.M., Patrial Netto, L., Hamerschmidt, R, 2020. Neural Recovery Function of the Auditory Nerve in Cochlear Implant Surgery: comparison between Prelingual and Postlingual Patients. Int. Arch. Otorhinolaryngol. 24, 444–449.

Cohen, L.T., 2009. Practical model description of peripheral neural excitation in cochlear implant recipients: 5. Refractory recovery and facilitation. Hear. Res. 248 (1–2), 1–14. doi:10.1016/j.heares.2008.11.004.

Crawley, M.J., 2012. The R book. John Wiley & Sons.

De Jong, M.A., Briaire, J.J., Biesheuvel, J.D., Snel-Bongers, J., Böhringer, S., Timp, G.R., Frijns, J.H., 2020. Effectiveness of Phantom Stimulation in Shifting the Pitch Percept in Cochlear Implant Users. Ear Hear. 41 (5), 1258–1269. doi:10.1097/AUD.0000000000001121.

Dong, Y., Briaire, J.J., Biesheuvel, J.D., Stronks, H.C., Frijns, J.H.M., 2020. Unravelling the Temporal Properties of Human eCAPs through an Iterative Deconvolution Model. Hear. Res. 395, 108037. doi:10.1016/j.heares.2020.108037.

Dong, Y., Stronks, H.C., Briaire, J.J., Frijns, J.H., 2021. An iterative deconvolution model to extract the temporal firing properties of the auditory nerve fibers in human eCAPs. MethodsX 8, 101240. doi:10.1016/j.mex.2021.101240.

Dynes, S.B.C., 1996. Discharge Characteristics of Auditory Nerve Fibers For Pulsatile Electrical Stimuli (Doctoral Dissertation. Massachusetts Institute of Technology.
Fitzmaurice, G.M., Laird, N.M., Ware, J., 2004. Linear mixed effects models. Appl. longitudinal Anal. 1, 187–236.
Fulmer, S.L., Runge, C.L., Jensen, J.W., Friedland, D.R., 2011. Rate of neural recovery in implanted children with auditory neuropathy spectrum disorder. Otolaryngol.-Head Neck Surg. 144 (2), 274–279. doi:10.1177/0194599810391603.
Gałecki, A., Burzykowski, T., 2013. Linear mixed-effects model. In: Linear Mixed-Effects Models Using R. Springer, New York, NY, pp. 245–273. doi:10.1007/978-1-4614-3900-4_13.
Gantz, B.J., Brown, C.J., Abbas, P.J., 1994. Intraoperative measures of electrically evoked AN compound action potential. Am. J. Otol. 15 (2), 137–144.
Gray, P.R., 1967. Conditional probability analyses of the spike activity of single neurons. Biophys. J. 7 (6), 759–777. doi:10.1016/S0006-3495(67)86621-9.
Gordon, K.A., Gilden, J.E., Ebinger, K.A., Shapiro, W.H., 2002. Neural response telemetry in 12-to 24-month-old children. Ann. Otol., Rhinol. Laryngol. 111 (5_suppl), 42–48. doi:10.1177/00034894021110S509.
Harrison, X.A., Donaldson, L., Correa-Cano, M.E., Evans, J., Fisher, D.N., Goodwin, C.E., … Inger, R., 2018. A brief introduction to mixed effects modelling and multi–model inference in ecology. PeerJ 6, e4794.
He, S., Teagle, H.F.B., Buchman, C.A., 2017. The electrically evoked compound action potential: from laboratory to clinic. Front. Neurosci. 11 (JUN), 1–20. doi:10.3389/fnins.2017.00339.
Holden, L.K., Finley, C.C., Firszt, J.B., Holden, T.A., Brenner, C., Potts, L.G., … Skinner, M.W., 2013. Factors affecting open-set word recognition in adults with cochlear implants. Ear Hear. 34 (3), 342. doi:10.1097/AUD.0b013e3182741aa7.
Kiefer, J., Hohl, S., Stürzebecher, E., Pfennigdorff, T., Gstöettner, W., 2001. Comparison of speech recognition with different speech coding strategies (SPEAK, CIS, and ACE) and their relationship to telemetric measures of compound action potentials in the nucleus CI 24M cochlear implant system. Int. J. Audiol. 40 (1), 32–42. doi:10.3109/00206090109073098.
Lai, W.K., Dillier, N., 2000. A Simple Two-Component Model of the Electrically Evoked Compound Action Potential in the Human Cochlea. Audiol. Neurotol. 5 (6), 333–345. doi:10.1159/000013899.
Lee, E.R., Friedland, D.R., Runge, C.L., 2012. Recovery from forward masking in elderly cochlear implant users. Otol. Neurotol. 33 (3), 355–363. doi:10.1097/MAO.0b013e318248ede5.
Matsuoka, A.J., Rubinstein, J.T., Abbas, P.J., Miller, C.A., 2001. The effects of interpulse interval on stochastic properties of electrical stimulation: models and measurements. IEEE Trans. Biomed. Eng. 48 (4), 416–424.
Miller, C.A., Abbas, P.J., Brown, C.J., 2000. An improved method of reducing stimulus artifact in the electrically evoked whole-nerve potential. In: Ear and Hearing, 21, pp. 280–290. doi:10.1097/00003446-200008000-00003.
Miller, C.A., Abbas, P.J., Robinson, B.K., 2001. Response properties of the refractory AN fiber. JARO - J. Assoc. Res. Otolaryngol. 2 (3), 216–232. doi:10.1007/s101620010083.
Molenberghs, G., Bijnens, L., Shaw, D., 1997. Linear Mixed Models and Missing Data. Linear Mixed Models in Practice. Lecture Notes in Statistics, 126. Springer, New York, NY doi:10.1007/978-1-4612-2294-1_5.
Morsnowski, A., Charasse, B., Collet, L., Killian, M., Müller-Deile, J., 2006. Measuring the refractoriness of the electrically stimulated AN. Audiol. Neurotol. 11 (6), 389–402. doi:10.1159/000095966.
Ramekers, D., Versnel, H., Strahl, S.B., Klis, S.F.L., Grolman, W., 2015. Recovery characteristics of the electrically stimulated AN in deafened guinea pigs: relation to neuronal status. Hear. Res. 321, 12–24. doi:10.1016/j.heares.2015.01.001.
Schielzeth, H., Dingemanse, N.J., Nakagawa, S., Westneat, D.F., Allegue, H., Teplitsky, C., … Araya-Ajoy, Y.G., 2020. Robustness of linear mixed-effects models to violations of distributional assumptions. Methods Ecol. Evol. 11 (9), 1141–1152. doi:10.1111/2041-210X.13434.
Shepherd, R.K., Hardie, N.A., 2001. Deafness-induced changes in the auditory pathway: implications for cochlear implants. Audiol. Neurootol. 6, 305–318.
Shepherd, R.K., Roberts, L.A., Paolini, A.G., 2004. Long-term sensorineural hearing loss induces functional changes in the rat auditory nerve. Eur. J. Neurosci. 20 (11), 3131–3140. doi:10.1111/j.1460-9568.2004.03809.x.
Strahl, S.B., Ramekers, D., Nagelkerke, M.M., Schwarz, K.E., Spitzer, P., Klis, S.F., … Versnel, H., 2016. Assessing the firing properties of the electrically stimulated auditory nerve using a convolution model. In: Physiology, Psychoacoustics and Cognition in Normal and Impaired Hearing. Springer, Cham, pp. 143–153. doi:10.1007/978-3-319-25474-6_16.
Stypulkowski, P.H., van den Honert, C., 1984. Physiological properties of the electrically stimulated AN. I. Compound action potential recordings. Hear. Res. 14 (3), 205–223 https://doi.org/10.1016/0378-5955(84)90051-0.
van den Honert, C., Stypulkowski, P.H., 1984. Physiological properties of the electrically stimulated auditory nerve. II. Single fiber recordings. Hear. Res. 14 (3), 225–243 https://doi.org/10.1016/0378-5955(84)90052-2.
Turner, C., Mehr, M., Hughes, M., Brown, C., Abbas, P., 2002. Within-subject predictors of speech recognition in cochlear implants: a null result. Acoust. Res. Lett. Online 3, 95–100. doi:10.1121/1.1477875.
van de Heyning, P., Arauz, S.L., Atlas, M., Baumgartner, W.D., Caversaccio, M., Chester-Browne, R., et al., 2016. Electrically evoked compound action potentials are different depending on the site of cochlear stimulation. Cochlear Implants Int 17, 251–262. doi:10.1080/14670100.2016.1240427.
Van Eijl, R.H.M., Buitenhuis, P.J., Stegeman, I., Klis, S.F.L., Grolman, W., 2017. Systematic review of compound action potentials as predictors for cochlear implant performance. Laryngoscope 127 (2), 476–487. doi:10.1002/lary.26154.
Wilson, B.S., Finley, C.C., Lawson, D.T., and Zerbi, M. (1994). Speech Processors for Auditory Prostheses. NIH Project N01-DC-2-2401. Seventh Quarterly Progress Report.
Xi, X., Ji, F., Han, D.Y., Huang, D.L., Hong, M.D., Yang, W.Y., 2004. Refractory recovery function of electrical auditory on the survival auditory nerve in cochlear implant recipients. Zhonghua Er Bi Yan Hou Ke Za Zhi 39 (2), 77–80.
Xu, J., Shepherd, R.K., Millard, R.E., Clark, G.M., 1997. Chronic electrical stimulation of the auditory nerve at high stimulus rates: a physiological and histopathological study. Hear. Res. 105 (1–2), 1–29. doi:10.1016/S0378-5955(96)00193-1.
Zhao, E.E., Dornhoffer, J.R., Loftus, C., Nguyen, S.A., Meyer, T.A., Dubno, J.R., McRackan, T.R., 2020. Association of patient-related factors with adult cochlear implant speech recognition outcomes: a meta-analysis. JAMA Otolaryngol.–Head Neck Surg. 146 (7), 613–620. doi:10.1001/jamaoto.2020.0662.